 Bull. Chem. Soc. Jpn., 75, 1031–1040 (2002)

Femtosecond/Picosecond Time-Resolved Spectroscopy of *trans*-Azobenzene: Isomerization Mechanism Following $S_2(\pi\pi^*) \leftarrow S_0$ Photoexcitation

Tatsuya Fujino, Sergei Yu. Arzhantsev, and Tahei Tahara[*,†]

Institute for Molecular Science (IMS), Myodaiji, Okazaki 444-8585

†The Institute of Physical and Chemical Research (RIKEN), 2-1 Hirosawa, Wako 351-0198

(Received September 25, 2001)

Photoisomerization dynamics and the electronic relaxation process of *trans*-azobenzene after the $S_2(\pi\pi^*) \leftarrow S_0$ photoexcitation were investigated in solution by femtosecond and picosecond time-resolved spectroscopy (UV-visible absorption, Raman, and fluorescence). Femtosecond time-resolved absorption spectrosocopy was performed to observe the transient absorption of the S_2 and S_1 states. Immediately after photoexcitation, a very broad transient absorption peaked at 475 and 600 nm was observed. This transient absorption decayed repidly within 0.5 ps, and this ultrafast component was attributed to the $S_n \leftarrow S_2(\pi\pi^*)$ absorption. After the decay of the S_2 state, a transient absorption showing peaks at 410 nm and 500 nm was observed, which was ascribable to the S_1 state. This transient absorption is similar to the $S_n \leftarrow S_1$ absorption that is observed after $S_1 \leftarrow S_0$ photoexcitation. Picosecond time-resolved Raman measurements were carried out to obtain information about the molecular structure of azobenzene in the S_1 state. The NN stretching frequency in the S_1 spectrum was determined with use of ^{15}N-substituted azobenzene, and it was found that the NN stretching frequency in the S_1 state is very close to that in the S_0 state (1428 cm^{-1} in the S_1 and 1440 cm^{-1} in the S_0). This fact indicated that the NN bond retains a double bond character in the S_1 state. A strong similarity was also found between the S_1 and S_0 Raman spectra. The double bond nature of the NN bond as well as the similarity between the S_1 and S_0 Raman spectra indicates that the observed S_1 state has a planar structure around the NN bond. The Raman data indicate that the observed S_1 state is not a twisted excited state that appears during the rotational isomerization, but is the excited state that is populated during the $S_2 \rightarrow S_1 \rightarrow S_0$ relaxation process while retaining a planar molecular structure. Anti-Stokes Raman measurements were performed to obtain information about the vibrational relaxation process. The anti-Stokes Raman spectra showed that the S_1 state was highly vibrationally excited. It was also observed that the hot bands due to the S_0 state appear after the decay of the S_1 state and these S_0 hot bands disappear with a time constant of ~16 ps in hexane. Femtosecond time-resolved and steady-state fluorescence measurements were performed and they revealed that the $S_2 \rightarrow$ "planar" S_1 relaxation process is the major relaxation pathway following S_2 photoexcitation. The quantum yield of the $S_2 \rightarrow$ "planar" S_1 electric relaxation was evaluated by comparing the intensity of the S_2 and S_1 fluorescence, and it was found to be almost unity. A series of time-resolved spectroscopy demonstrated that the S_2 rotational isomerization mechanism, which had been believed so far, does not exist. It has been clarified that the isomerization occurs in the S_1 state after $S_2 \rightarrow S_1$ relaxation. Consequently, it is concluded that the isomerization of azobenzene takes place in the S_1 state by inversion in cases of both S_2 and S_1 photoexcitation.

Azobenzene is a well-known molecule that shows photoisomerization. The *cis-trans* photoisomerization of this molecule is very important not only from the viewpoint of fundamental photochemistry but also for its high potential in industrial applications.[1–3] The elucidation of the mechanism and dynamics of the isomerization reaction is a central issue for the photochemical study of this molecule. However, the mechanism and dynamics have not been well clarified because the reaction of azobenzene takes place very rapidly.

It has been well established for olefinic molecules that $\pi\pi^*$ excitation induces rotational isomerization around the C=C double bond.[4–7] However, the isomerization around N=N double bond in azobenzene has been considered to occur with a different mechanism, especially when the molecule is excited to the $n\pi^*(S_1)$ state. Rau and Lüddecke synthesized azobenzene derivatives in which the rotational motion is prohibited, but they found that the isomerization quantum yield was equivalent to that of azobenzene itself in the case of $S_1(n\pi^*)$ excitation.[8] So, they proposed that isomerization after $n\pi^*$ excitation proceeds not with rotation around the N=N bond but with inversion around a N atom. As for the isomerization after $\pi\pi^*(S_2)$ excitation, the excitation wavelength dependence of *trans* → *cis* isomerization quantum yield has been examined and it was found that the quantum yield obtained with S_2 excitation (~0.1) is significantly different from that with $S_1(n\pi^*)$ excitation (~0.2).[9–11] On the basis of this difference, the isomerization mechanism after S_2 excitation was claimed to be different from that after S_1 excitation. Consequently, it has been considered that azobenzene undergoes two different isomerization processes depending on the excitation wave-

length: with $S_1(n\pi^*) \leftarrow S_0$ excitation, the isomerization occurs with the inversion around a N atom (the inversion mechanism), whereas the rotation around the NN double bond is induced by $S_2(\pi\pi^*) \leftarrow S_0$ excitation (the rotation mechanism) (Scheme 1). A low-level quantum chemical calculation also provided potential curves that looked consistent with this reaction scheme.[12] Therefore, the isomerization scheme shown in Scheme 1 had been accepted for a long time. At close inspection, however, there has been no experimental evidence that directly supports the existence of the rotational isomerization after $S_2(\pi\pi^*)$ excitation, while inversion in the S_1 state was strongly indicated by the experiments of Rau and Lüddecke.

Time-resolved spectroscopy is the most powerful tool to study photochemical dynamics. However, it is only recently that time-resolved spectroscopy was applied to the study of photoisomerization of azobenzene. Lednev et al. conducted femtosecond UV-visible absorption spectroscopy with $S_2(\pi\pi^*) \leftarrow S_0$ photoexcitation to clarify photoisomerization dynamics of *trans*-azobenzene.[13–15] In their time-resolved absorption measurements, a transient band assignable to the $S_2(\pi\pi^*)$ state was first observed around ~475 nm. After it decays (< 200 fs), another transient absorption was observed around ~400 nm whose lifetime is ~1 ps in hexane. In addition, a minor slowly decaying component having a lifetime of ~16 ps was also observed around ~400 nm. Lednev et al. assigned the transient absorption observed around ~400 nm to the twisted excited states in the S_2 (lifetime ~1 ps) and S_1 (~16 ps) states that are supposed to appear during the rotational isomerization. Meanwhile, Nägele et al. performed time-resolved absorption study of the *cis* isomer that exists in the photostationary *cis*/*trans* balance.[16] They found that photoisomerization from the *cis* isomer proceeds with a time constant of ~170 fs with $S_1(n\pi^*)$ excitation (435 nm). The vibrational cooling process in the electronically ground state was also studied by Hamm et al., using time-resolved infrared spectroscopy. It was concluded that the intermolecular energy transfer to the surrounding solvent takes place on a time scale of ~20 ps.[17] These spectroscopic studies have provided important information about the photochemical dynamics of azobenzene. However, all these spectroscopic data have been interpreted *within* the framework of the reaction scheme shown in Scheme 1.

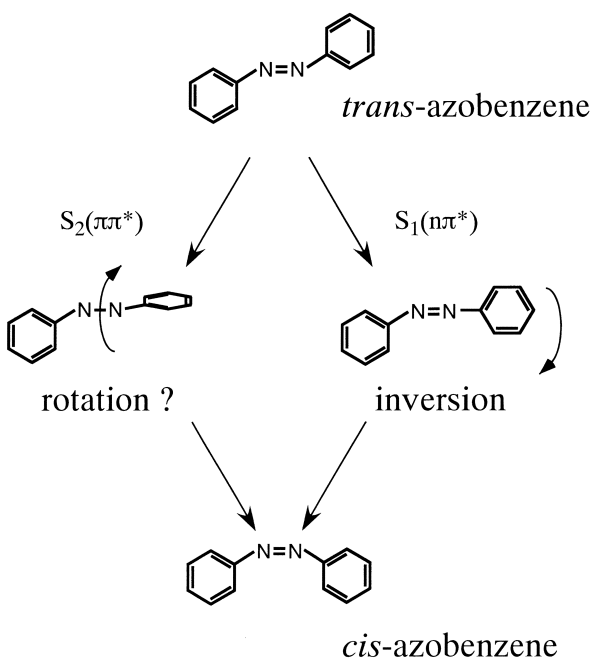

Scheme 1.

We recently studied photoisomerization of *trans*-azobenzene after $S_2(\pi\pi^*) \leftarrow S_0$ photoexcitation using picosecond time-resolved Raman and femtosecond fluorescence spectroscopies.[18,19] The picosecond Raman study demonstrated that the $S_2 \rightarrow S_1 \rightarrow S_0$ relaxation observed after S_2 photoexcitation is the process taking place in the molecule that retains essentially planar structure around the NN bonding.[18] Moreover, the femtosecond time-resolved fluorescence spectroscopy clarified that the photoexcited S_2 state is almost exclusively relaxed to the "planar" S_1 state and that the rotational isomerization pathway starting directly from the $S_2(\pi\pi^*)$ state does not exist.[18] This series of our works requested essential revision of the photoisomerization scheme of *trans*-azobenzene that had been employed so far.

The above-described situation urged us to re-examine time-resolved absorption of *trans*-azobenzene, since the absorption data were claimed to support the rotational isomerization pathway in the S_2 state.[13–15] In fact, it is now very necessary to discuss all the data taken by different time-resolved spectroscopies in a unified and consistent framework. In this paper, we describe the results of the three time-resolved spectroscopies, femtosecond absorption, picosecond Raman and femtosecond fluorescence spectroscopies, all of which were carried out in our laboratory. The aim of this paper is to construct a solid picture of the photochemical dynamics of *trans*-azobenzene following $S_2(\pi\pi^*)$ excitation, by gathering pieces of information provided by each spectroscopy. It will be shown that the isomerization of *trans*-azobenzene takes place in the S_1 state, most likely by inversion, regardless of differences in the initial photoexcitation.

Experimental Section

Femtosecond Time-Resolved UV-Visible Absorption Measurements. The apparatus used for transient absorption measurements has been described elsewhere.[20] The output of a mode-locked Ti:sapphire laser (800 nm, 8 nJ, 65 fs, 78 MHz; Coherent, MIRA-900F) pumped by an Ar^+ laser (Coherent, INNOVA310) was amplified to an energy of ~1 mJ with a regenerative amplifier (Clark-MXR, CPA-1000, operated at 100 Hz). The third harmonics (~20 μJ) of the amplified pulse or the sum frequency between the amplified pulse and the output from an OPA system (Quantronix, TOPAS) was used as pump. The white-light continuum generated from D_2O was used as probe. The probe beam was focused on a thin film-like jet stream of a sample solution, and it was spatially overlapped with the pump beam. The time delay between the pump and probe pulses was controlled with an optical delay line. The polarization of the probe beam was set at the magic angle to that of the pump beam. The probe intensity with/without pump irradiation was monitored by a polychromator (CHROMEX, 500im) equipped with a CCD detector (Princeton Instruments, TEA/CCD-1024-EM/1UV). Pulse-to-pulse fluctuation of the probe beam was corrected for each laser shot by moni-

toring the reference intensity. The Kerr gate signals from hexane solution were measured under the same experimental condition, and the group-delay dispersion of the probe light was corrected on the basis of the obtained Kerr data. The time resolution of the measurements was also evaluated from the Kerr data, which was typically 600–700 fs.

Picosecond Time-Resolved Raman Measurements. The experimental setup for the picosecond time-resolved Raman measurements has already been described.[7] Briefly, the third harmonics (273 nm) of the output of a regeneratively amplified Ti:sapphire laser (Spectra-Physics, 0.8 mJ, 1 kHz) was focused onto a sample solution for photoexcitation. The second harmonics (410 nm) of the output of the Ti:sapphire laser was used to probe spontaneous Raman scattering. The polarization between the pump and probe pulses was set parallel. The Raman signals from the sample solution were analyzed with a polychromator (Jovin-Yvon, HR-320) and detected by a liquid nitrogen-cooled CCD detector (Princeton Instruments, LN/CCD-1100PB). The Kerr gate signal from heptane was measured to determine the delay time origin as well as the time resolution of the measurements (~2.8 ps).

Femtosecond Time-Resolved and Steady-State Fluorescence Measurements. Femtosecond time-resolved fluorescence was measured using the apparatus described previously.[21,22] The third harmonic pulses (280 nm, 560 pJ) of a mode-locked Ti:sapphire laser (Spectra-Physics, Tsunami) were used for photoexcitation of the sample. The residual fundamental pulses after the third harmonic generation were used as gate pulses for the fluorescence up-conversion process. The up-converted fluorescence signal was separated by a monochromator (Jovin-Yvon, HR-320) and detected by a photomultiplier (Hamamatsu, H585) with a photon counter (Stanford Research Systems, SR400). The polarization of excitation and detection was set at the magic angle. The time resolution of the fluorescence up-conversion measurements was evaluated by the cross correlation between the excitation and gate pulses, the value was typically ~230 fs (FWHM). All the measurements were performed at room temperature.

Steady-state fluorescence spectrum was measured with use of the detection system in the picosecond Raman apparatus. The steady-state measurement was also carried out under the magic angle condition. Sensitivity correction of the detection system was done using a standard lamp (Ushio, 3230 K color temperature). The spectral distortion due to the self-absorption effect was corrected.

Sample Preparations. Azobenzene (*trans*) was purchased from Wako Pure Chemical Industries and it was recrystallized three times from methanol. ^{15}N-substituted azobenzene, $(C_6H_6{}^{15}N)_2$, was synthesized and purified according to the literature.[23] Both samples, normal and isotopic substituted azobenzene, were sufficiently dried in a dry box before use. Hexane was purchased from Wako Pure Chemical Industries (HPLC grade) and used as received. The solution with a concentration of 5.0×10^{-3} (absorption, fluorescence) or 1.5×10^{-2} mol dm^{-3} (Raman) was used for time-resolved measurements. A fresh sample solution was prepared for each measurement.

Results and Discussions

Femtosecond Time-Resolved Absorption: Kinetics of Relaxation After S_2 Photoexcitation. The electronically ground state of *trans*-azobenzene (we simply call it azobenzene hereafter) shows two absorption bands in the UV-visible region. A strong band around ~300 nm is assigned to the S_2-($\pi\pi^*$) ← S_0 transition whereas another weak band around ~450 nm is ascribed to the S_1 ($n\pi^*$) ← S_0 transition. The pumping wavelength (267nm) for the time-resolved absorption measurements corresponds to the blue side of the S_2 ← S_0 absorption, and the molecules are initially photoexcited to the S_2-($\pi\pi^*$) state. The transient absorption spectra obtained from a hexane solution (5.0×10^{-3} mol dm^{-3}) are shown in Fig. 1(a) for the delay time range from −1 to 100 ps. Immediately after photoexcitation, a very broad transient absorption that covers the whole visible region appears. Then a broad "offset-like" absorption showing peaks at 475 and 600 nm decays rapidly within 0.5 ps. This ultrafast component is attributable to the S_n ← $S_2(\pi\pi^*)$ absorption.[14] The observed S_2 spectrum is noticeably different from that reported by Lednev et al.[14] (especially for the existence of the broad "offset-like" feature and the peak at 600 nm) while it is very similar to the reported S_2 spectrum of an azobenzene derivative (*trans*-4-butyl-4′-methoxyazobenzene).[24] With the rapid decay of the broad S_2 absorption, a transient absorption showing peaks at 410 nm and 500 nm is

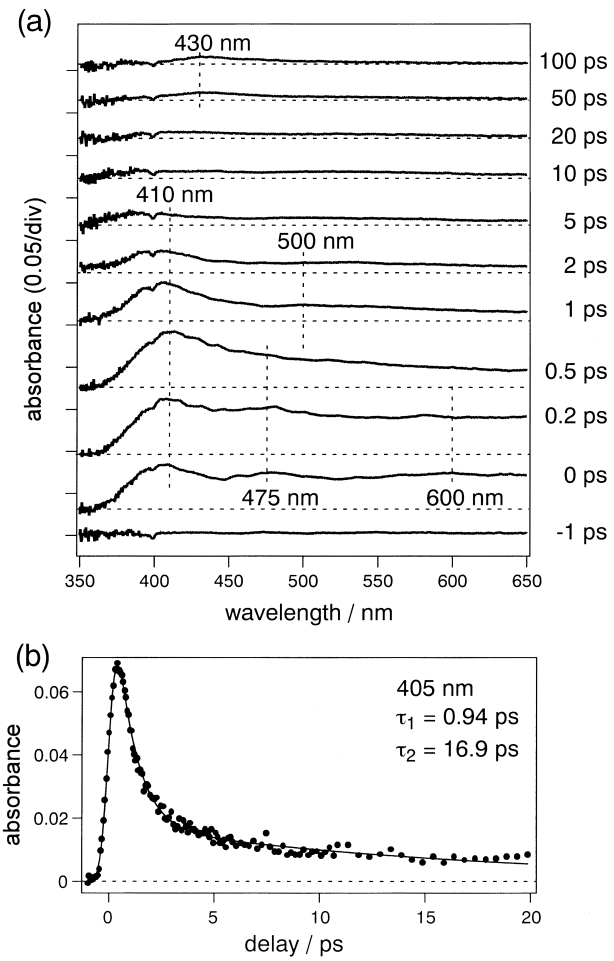

Fig. 1. (a) Femtosecond time-resolved UV-visible absorption spectra of azobenzene in hexane in the delay time range from −1 to 100 ps (5.0×10^{-3} mol dm^{-3}; pump laser 267 nm). (b) Temporal behavior of transient absorption at 405 nm. The dotted circles are the experimental data and the solid line is the best-fit curve having a decay time constants of $\tau_1 = 0.94$ and $\tau_2 = 16.9$ ps.

observed. This second absorption is ascribable to the transient species generated from the S_2 state, although its rise was not fully time-resolved in the present measurement owing to the limited time resolution. This transient absorption band becomes prominent after ~0.5 ps and then it decays with increase of the delay time.

The temporal change of the absorbance at 405 nm is depicted in Fig. 1(b) for the delay time range from −1 to 20 ps. The observed decay was well fitted by a double exponential function convoluted with the instrumental response, and two time constants of $\tau_1 = 0.94$ ps and $\tau_2 = 16.9$ ps were evaluated.[25] The kinetics observed at 405 nm is essentially the same as that reported by Lednev et al., who used 303 and 280 nm excitation.[13,14] The main decay component, $\tau_1 = 0.94$ ps, represents the lifetime of the transient species that is generated from the S_2 state. Lednev et al. assigned this component to the "twisted" S_2 state.[13–15] However, we later found that its lifetime strongly depends on the solvent and that it becomes ~13 ps in ethylene glycol.[18] Since it is very unlikely that the S_2 state has a lifetime as long as 13 ps, the 410-nm transient showing the τ_1 decay should be assigned to the S_1 state of azobenzene. The minor decay component in the absorbance change ($\tau_2 = 16.9$ ps) is not due to the decay of the S_1 state. As seen in Fig. 1(a) the time-resolved spectra corresponding to this component (e. g., the spectrum at 5 ps) do not show any peak around ~410 nm and exhibit significantly different spectral features. In the previous study, this τ_2 component was assigned to the "twisted" S_1 state.[13–15] However, time-resolved anti-Stokes Raman spectroscopy clearly shows that it originates from the vibrational cooling process taking place in the S_0 state, as described in detail in the next section. In other words, the transient feature showing the τ_2 decay is attributed to the spectral change of the S_0 absorption that accompanies the vibrational cooling process in the S_0 states.

In Fig. 1(a), we note that a very weak absorption remains around ~430 nm after all the prominent transient absorption bands disappear. This weak feature ($\Delta A \sim 0.01$) is very long-lived and its decay was not recognized in the measured delay time range up to 100 ps. This band is highly likely assignable to the absorption of the *cis* isomer that is produced by photoisomerization. (More strictly speaking, it corresponds to the absorption difference between *cis*- and *trans*-azobenzene in the S_0 state.) It is known that *cis*-azobenzene exhibits the $S_1(n\pi^*) \leftarrow S_0$ absorption peaked around ~430 nm ($\varepsilon_{430}^{cis} \approx 1500$ mol^{-1} dm^3 cm^{-1}, $\varepsilon_{430}^{trans} \approx 500$ mol^{-1} dm^3 cm^{-1}). The absorbance change induced at 430 nm by *trans* → *cis* photoisomerization can be estimated as $\Delta\mathrm{OD} \approx (\varepsilon_{430}^{cis} - \varepsilon_{430}^{trans})Cl\Phi$, where C and l correspond to the sample concentration and thickness, respectively, and Φ is the quantum yield of *trans* → *cis* photoisomerization after S_2 photoexcitation. Using 5.0×10^{-3} mol dm^{-3} for C, 200 μm for l and 0.11 for Φ (in hexane), we obtained the ΔOD value of ~0.011. The estimated ΔOD value accords well with the observed transient absorbance at 430 nm, which supports our assignment.

When we discuss the isomerization pathway after S_2 excitation based on the time-resolved absorption data, a key is the S_1 state that exhibits transient absorption around ~410 nm. In order to consider this transient further, it is desirable to compare its spectrum with the S_1 spectrum obtained by direct $S_1 \leftarrow S_0$ excitation. Thus, we carried out the femtosecond time-resolved absorption measurement also with direct $S_1(n\pi^*) \leftarrow S_0$ excitation.

The transient absorption spectrum obtained with direct $S_1 \leftarrow S_0$ excitation from a hexane solution is shown in Fig. 2(a). The pumping wavelength (500 nm) for this measurement corresponds to the red side of the $S_1 \leftarrow S_0$ absorption. The transient absorption shown here appeared immediately after photoexcitation, weakened with increasing delay time, and then completely vanished after 5 ps. Therefore, this transient absorption can be straightforwardly ascribed to the S_1 state. In Fig. 2(b), the S_1 absorption observed at 1 ps after S_2 photoexcitation is depicted for comparison. The spectral feature of the S_1 spectrum obtained by direct S_1 excitation is very similar to that observed after S_2 excitation, but there are some differences: (1) A very broad offset-like feature is absent, (2) the peak position of the most prominent band around 400 nm is blue-shifted (i. e., 410 nm → 400 nm), and (3) the width of this band is significantly narrower. It should be noted that the lifetime of the S_1 state is also different between S_1 and S_2 excitations.[14] Because of these differences, it was argued that the 410-nm transient that appears after S_2 photoexcitation is not the S_1 state populated by direct $S_2 \leftarrow S_0$ photoexcitation, in the previous time-resolved absorption studies.[13–15]

Time-resolved absorption data afford crucial information about the kinetics of the relaxation process of photoexcited azobenzene. However, unambiguous assignment of each transient species cannot be made only by the transient absorption data, so that the obtained data cannot be fully interpreted. Full understanding of the observed time-resolved spectroscopic data can be gained by combining information of femtosecond absorption spectroscopy and picosecond Raman spectroscopy, as described in the following subsections. In fact, it is clearly shown that the above-described difference in S_1 absorption spectrum is due to the difference in vibrational excess energy, and that the S_1 state appearing after S_2 and S_1 photoexcitation is essentially the same, as which is the "planar" S_1 state.

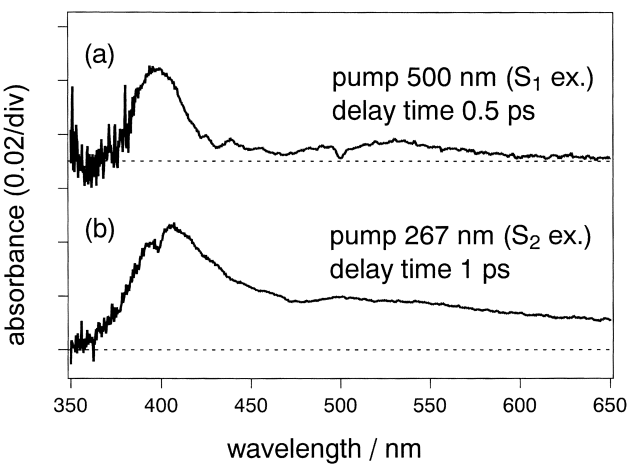

Fig. 2. (a) Femtosecond time-resolved UV-visible absorption spectra of azobenzene in hexane: (a) with $S_1 \leftarrow S_0$ photoexcitation (500 nm) at 0.5 ps delay time, (b) with $S_2 \leftarrow S_0$ photoexcitation (267 nm) at 1 ps delay time.

Picosecond Time-Resolved Raman Scattering: Molecular Structure of the S_1 State and Vibrational Cooling Process. When we consider the S_1 state (the 410-nm transient) appearing after S_2 photoexcitation, the information about the molecular structure is crucial. If femtosecond absorption spectroscopy sees the rotational isomerization pathway starting from the S_2 state, it is expected that the S_1 state generated from the S_2 state has a twisted structure around N=N double bond. Actually, the first interpretation about femtosecond time-resolved absorption data was made in this context.[13–15] However, transient absorption affords little information about the molecular structure, so that we could not make any clear arguments about isomerization pathway based only on time-resolved absorption data. Time-resolved resonance Raman spectroscopy often affords unique information that cannot be obtained by other types of spectroscopy. Raman spectra contain rich information about the molecular structure, and time-resolved anti-Stokes measurements give clear information about the vibrational relaxation process. We thus carried out picosecond time-resolved Raman measurements to obtain information about the molecular structure of the S_1 state that appears after S_2 excitation.

In time-resolved Raman measurements, we used excitation at 273 nm to excite molecules to the $S_2(\pi\pi^*)$ state. The probe wavelength at 410 nm is in resonance with the $S_n \leftarrow S_1$ transient absorption peaked at 410 nm. The procedure to obtain the transient Raman spectra was as follows. In the spectrum taken with the pump and probe irradiation, Raman scattering was observed on the fluorescence background. We subtracted fluorescence background from the spectrum using the fluorescence spectrum measured with only pump irradiation. Then, we carefully subtracted Raman bands of S_0 azobenzene and solvent, and obtained the Raman spectrum of S_1 azobenzene. The S_1 Raman signals were so weak that we needed a careful subtraction to obtain a reliable S_1 spectrum. In the Fig. 3(a), we depict the picosecond transient Raman spectrum of the S_1 state, which was obtained from an ethylene glycol solution (1.5×10^{-2} mol dm^{-3}) at the delay time of 0 ps. Ethylene glycol was used as solvent since the lifetime of the S_1 state becomes significantly longer.

The vibrational frequency of a characteristic normal mode is very sensitive to the structural change of the molecule. For S_1 azobenzene, structural information around the central NN bond is very important, and hence determination of the NN stretching frequency is crucial. In order to find the NN stretch band in the S_1 Raman spectrum, we synthesized a ^{15}N-isotopic analogue, in which both of the two N atoms are substituted by ^{15}N, and then measured Raman spectra of the S_1 state. Figure 3(b) shows the S_1 Raman spectrum of ^{15}N-substituted azobenzene. For comparison, the Raman spectrum of the S_0 state is also shown for the ^{14}N normal species in Fig. 3(c). In the S_0 Raman spectrum, the strongest Raman band at 1440 cm^{-1} showed a large isotopic shift ($\sim$29 cm^{-1}) by the ^{15}N substitution (not shown). The observed isotopic shift agrees well with the literature,[26] and the 1440 cm^{-1} band is ascribed to the NN stretching vibration in the S_0 state. In the S_1 spectra, on the other hand, the Raman band at 1428 cm^{-1} shows a 27-cm^{-1} downshift by the ^{15}N substitution (Figs. 3(a) and 3(b)). Therefore, the 1428-cm^{-1} band can be assigned to the NN stretching vibration in the S_1 state. The ^{15}N shift for the S_1 band at 1428 cm^{-1} is almost the same as that for the S_0 band at 1440 cm^{-1} (27 cm^{-1} in S_1 and 29 cm^{-1} in S_0). It implies that the corresponding vibrational modes are similar to each other.

The NN stretching frequency in the S_1 state (1428 cm^{-1}) is very close to that in the S_0 state (1440 cm^{-1}). This small frequency difference (12 cm^{-1}) in the NN stretching frequency

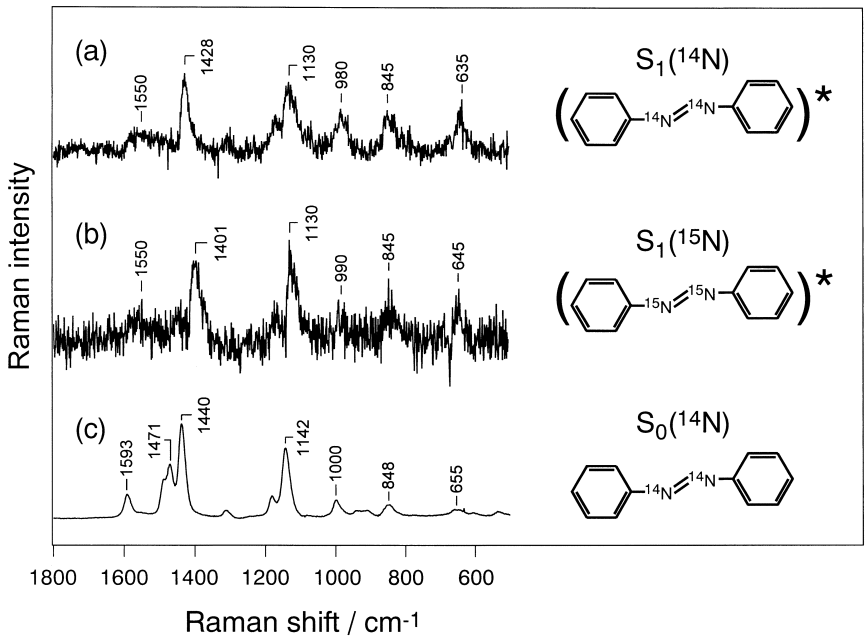

Fig. 3. Raman spectra of azobenzene in the S_1 and the S_0 state in ethylene glycol solution. Normal (^{14}N) species in the S_1 state (a), ^{15}N analogue in the S_1 state (b), and normal species in the S_0 state (c). The S_1 Raman spectra were taken at 0 ps delay time.

indicates that the structural change around the NN bond is very small and that the NN bonding retains a double bond character in the S_1 state. We also found very strong similarity between the S_1 and S_0 Raman spectral features. These observations strongly indicate that the observed S_1 state is not a twisted excited state but has a planar structure around the central NN bond. One may expect a significant structural shift in the S_1 state alond some coordinate because photoexcited azobenzene shows very fast *trans* → *cis* isomerization. However, the present Raman data revealed that this coordinate is not torsion around the NN bond.

In femtosecond time-resolved absorption measurements, we observed a transient species that decays with a lifetime of ~17 ps in hexane (the τ_2 component). Picosecond time-resolved Raman measurements also afford crucial data that enable us to make a clear assignment of this component.

Picosecond time-resolved anti-Stokes Raman spectra measured from a hexane solution are shown in Fig. 4. The Raman signals observed only with probe irradiation were already subtracted, and the Raman intensity at each delay time was normalized using the solvent Raman intensity. Immediately after photoexcitation, several anti-Stokes transient Raman bands were observed at 1425, 1120, 985, 850 and 650 cm^{-1} and they vanish within a few picoseconds (Fig. 4(a)). These anti-Stokes Raman bands are assignable to the S_1 state of azobenzene. It should be noted that the high frequency anti-Stokes Raman bands appear with fairly high intensity, which implies that the observed S_1 state is highly vibrationally excited after $S_2 \rightarrow S_1$ electronic relaxation. After the decay of these S_1 Raman bands, anti-Stokes Raman bands at 1440 and 1128 cm^{-1} remain (Fig. 4(b)). Although the band shapes of these bands are slightly broadened, these Raman frequencies are almost identical to the N=N stretch and the C–N stretch bands of S_0 azobenzene. Thus, these anti-Stokes Raman bands are assigned to the vibrationally hot S_0 state. With photoexcitation at 273 nm, the molecule gains the energy greater than 36000 cm^{-1}. The lifetimes of the S_2 and S_1 states are so short in hexane that a considerable amount of the photoexcitation energy is expected to be still localized in the azobenzene molecule after the $S_2 \rightarrow S_1 \rightarrow S_0$ electronic relaxation. Therefore, it is very natural to observe the vibrationally hot S_0 state in picosecond time-resolved anti-Stokes Raman measurements in hexane. The S_0 anti-Stokes Raman bands disappear with a time constant of ~16 ps, which corresponds to the vibrational cooling process in the S_0 state (the energy dissipation to the surrounding solvent). This time constant (16 ps) is exactly the same as the lifetime of the τ_2 component found in time-resolved absorption measurements, which implies that their origins are the same. Picosecond time-resolved anti-Stokes Raman measurements disclosed that the slowly decaying τ_2 component seen at 405 nm arises from the vibrational cooling process in the S_0 state.

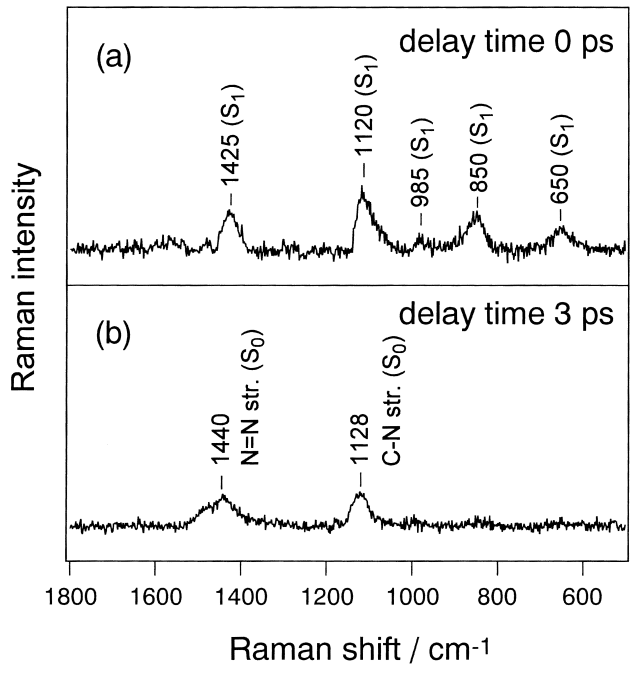

Fig. 4. Picosecond time-resolved anti-Stokes Raman spectra of azobenzene in hexane taken at 0 ps and 3 ps. The Raman intensity at each delay time has been normalized using the solvent band intensity.

By combining the information of femtosecond time-resolved absorption spectroscopy and picosecond time-resolved Raman spectroscopy, we can conclude that the process seen in the time-resolved spectroscopy is the $S_2 \rightarrow$ hot "planar" $S_1 \rightarrow$ hot $S_0 \rightarrow S_0$ relaxation process, but not the rotational isomerization process starting from the S_2 state. Raman spectroscopy clearly showed that the S_1 state generated from the S_2 state has a planar structure, which means that the relevant S_1 potential minimum is located rather closely to the potential minimum of the S_0 state. Such a result implies that the S_1 state generated after S_2 excitation is the same S_1 state that is populated by direct $S_1 \leftarrow S_0$ photoexcitation, because the optical transition takes place vertically. (Nevertheless, the vibrational excess energy in the S_1 state is different between S_2 and S_1 photoexcitation). It has been experimentally demonstrated that the inversion isomerization takes place with direct $S_1 \leftarrow S_0$ photoexcitation.[8] Consequently, the "planar" S_1 state observed after $S_2 \leftarrow S_0$ photoexcitation is considered to be the state from which the inversion isomerization starts. Proper interpretation of time-resolved absorption and Raman data lead us to think that the inversion isomerization in the S_1 state takes part also in the isomerization following the S_2 photoexcitation. The time-resolved spectroscopic data certainly request the revision of the reaction Scheme 1, in which the S_2 excitation induces rotational isomerization without relaxation to the "planar" S_1 state and the *cis* isomer is produced exclusively from the twisted excited-state intermediate.

Steady-State and Time-Resolved Fluorescence: the Quantum Yield of the $S_2 \rightarrow$ "planar" S_1 Relaxation and Clarification of the Major Isomerization Pathway. As described above, the time-resolved absorption and Raman data disclosed that the "planar" S_1 state is generated after S_2 excitation. They also indicated that inversion isomerization in the S_1 state takes part in the isomerization following the S_2 excitation. However, this finding, by itself, cannot exclude the existence of the rotational isomerization pathway starting from the S_2 state, because it cannot exclude the possibility that the relaxation pathway to the "planar" S_1 state is a minor process and that a significant number of molecules are still relaxed through

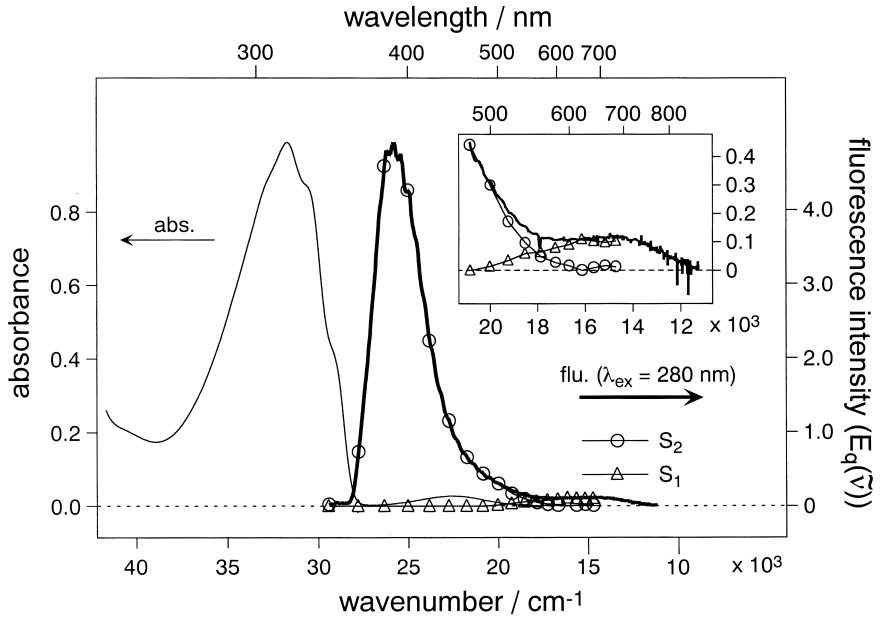

Fig. 5. The absorption spectrum (left) and the steady-state fluorescence spectrum obtained with 280-nm excitation (right). The fluorescence intensity is represented as the photon number intensity in the frequency space. In the fluorescence spectrum, the open circles and the open triangles represent the decomposition into the S_2 and S_1 fluorescence, respectively. The wavenumber region from 22000 to 12000 cm^{-1} is expanded in the inset.

the rotational pathway which is totally "dark" in the time-resolved absorption and Raman measurements. Therefore, we need to clarify which is the major isomerization pathway after S_2 excitation, the rotational isomerization starting directly from the $S_2(\pi\pi^*)$ state, or the inversion isomerization that takes place from the "planar" S_1 state after the $S_2 \rightarrow S_1$ relaxation. We carried out steady-state and femtosecond time-resolved fluorescence measurements to obtain a clear answer for this question by determining the $S_2 \rightarrow$ "planar" S_1 relaxation quantum yield.

Figure 5 depicts steady-state fluorescence spectrum taken from a hexane solution (5.0×10^{-3} mol dm^{-3}) with the $S_2(\pi\pi^*) \leftarrow S_0$ photoexcitation at 280 nm. The UV-visible absorption spectrum is also shown in this figure for comparison. The intensity maximum of the steady-state fluorescence was observed around ~390 nm (~25750 cm^{-1}), and it is energetically higher than the $S_1(n\pi^*) \leftarrow S_0$ transition. This main fluorescence band shows a mirror image of the $S_2(\pi\pi^*) \leftarrow S_0$ absorption band, so that we assigned it to the S_2 fluorescence band. The fluorescence spectrum extends to the red region and it exhibits a very weak peak around ~665 nm (~15000 cm^{-1}). This second fluorescence band shows a mirror image of the $S_1(n\pi^*) \leftarrow S_0$ absorption band, and hence it is assignable to the S_1 fluorescence. The appearance of the S_1 fluorescence showing a mirror image of the $S_1(n\pi^*) \leftarrow S_0$ absorption demonstrates that the S_1 state that is Franck–Condon active from the S_0 state is certainly generated after the S_2 excitation. In other words, the observed S_1 fluorescence is assignable to the fluorescence from the "planar" S_1 state.

Femtosecond time-resolved fluorescence measurements were carried out in the wavelength region from 340 to 680 nm by the up-conversion method. The time-resolved fluorescence traces are shown in Fig. 6. The temporal behavior of the fluo-

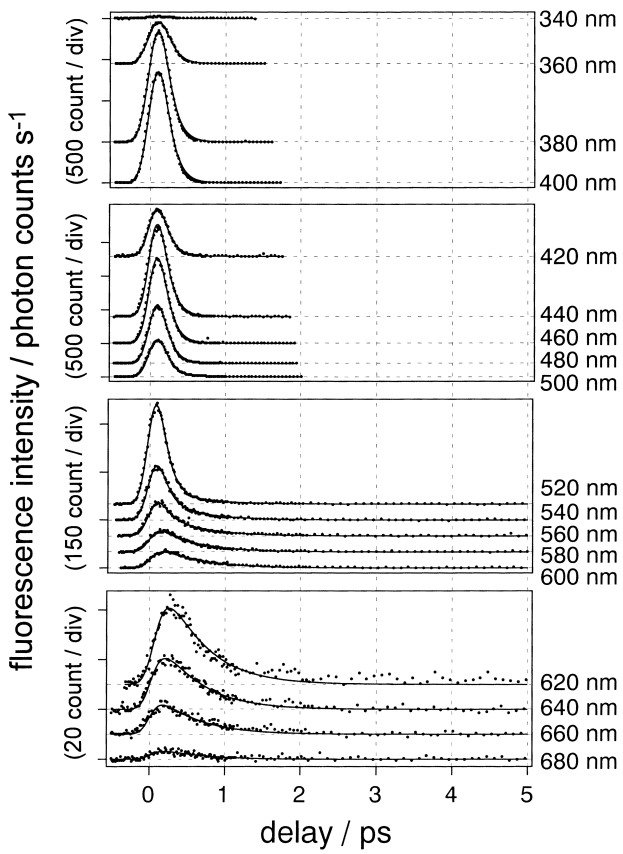

Fig. 6. Femtosecond time-resolved fluorescence signals obtained from azobenzene in hexane (5.0×10^{-3} mol dm^{-3}; pump laser 280 nm) in the wavelength region from 340 nm to 680 nm. The dotted circles are the experimental data, and solid curves are the results of the fitting analysis.

rescence signals varies with the change of wavelength, reflecting the dual nature of the fluorescence. In the S_2 fluorescence region (340–500 nm), we observed very rapid decay that is comparable to the instrumental response. The second slower fluorescence component becomes noticeable in the longer wavelength region. In the decay around 580 nm, the amplitude of the second component becomes comparable to that of the first component, and then it becomes predominant around 640 nm in the S_1 fluorescence region. Considering the observed temporal behavior and steady-state fluorescence spectrum, we can straightforwardly assign the first (fast) and second (slow) components to the S_2 and S_1 fluorescence, respectively. The time-resolved fluorescence signals decayed to the dark level within 5 ps, indicating that there is no other long-lived fluorescent state.

In order to obtain quantitative information, the time-resolved fluorescence data were analyzed on the basis of the following relaxation scheme:

$$\begin{array}{l} S_2 \xrightarrow{k_{vert}} S_1 \xrightarrow{k_{S_1}} \\ \qquad\quad \searrow^{k_{ROT}} \end{array} \qquad (1)$$

Since the observed fluorescence consists of the S_2 fluorescence ($R_{S2}(\tilde{\nu}, t)$) and the S_1 fluorescence ($R_{S1}(\tilde{\nu}, t)$), the time-resolved fluorescence intensity can be described as follows:

$$\begin{aligned} R(\tilde{\nu}, t) &= R_{S2}(\tilde{\nu}, t) + R_{S1}(\tilde{\nu}, t), \\ &= a_{S2}(\tilde{\nu})\exp(-k_{S2}t) + a_{S1}(\tilde{\nu})\Phi\, k_{S2}/ \\ &\quad (k_{S2} - k_{S1})\{\exp(-k_{S1}t) - \exp(-k_{S2}t)\}, \end{aligned} \qquad (2)$$

where

$$k_{S2} = k_{vert} + k_{ROT},\ \Phi = k_{vert}/(k_{vert} + k_{ROT}).$$

In this expression, $a_{S2}(\tilde{\nu})$ and $a_{S1}(\tilde{\nu})$ denote the transition probabilities of the two excited states at wavenumber $\tilde{\nu}$, whereas k_{S2} and k_{S1} represent their population relaxation rates. Note that the k_{S2} rate is the sum of the $S_2 \rightarrow S_1$ relaxation (k_{vert}) and other relaxation pathways (k_{ROT}) that include the rotational isomerization in the S_2 state as well as the direct non-radiative $S_2 \rightarrow S_0$ relaxation. Therefore, the Φ value represents the quantum yield of the $S_2 \rightarrow$ "planar" S_1 relaxation process. By a fitting analysis, we obtained the S_2 and S_1 lifetimes as 0.11 ps ($1/k_{S2}$) and 0.50 ps ($1/k_{S1}$), respectively. The best fits obtained with these lifetimes are shown by solid curves in Fig. 6. The S_1 lifetime determined by the time-resolved fluorescence data was shorter than the value obtained from the time-resolved absorption data (0.94 ps). We consider that the value determined from fluorescence data is more reliable, because (1) the time resolution of the up-conversion measurements ($\sim$230 fs) is much better than that of absorption experiments (600–700 fs), and (2) the absortion data contain contributions from not only S_1 absorption but also S_0 spectral change (e. g. bleaching and cooling). In addition to the lifetime, we also determined the amplitude of each component, $a_{S2}(\tilde{\nu})$ and $a_{S1}(\tilde{\nu})\Phi$, which represent the contribution of the S_2 and S_1 fluorescence at each wavelength. By plotting these parameters after normalization, we could successfully decompose the steady-state fluorescence spectrum into the S_2 and S_1 fluorescence components, as shown in Fig. 5.

The quantitative analysis of time-resolved fluorescence as well as the decomposition of the fluorescence spectrum enables us to determine the quantum yield of the $S_2 \rightarrow$ "planar" S_1 relaxation process (Φ) by comparing the intensities of the S_2 and S_1 fluorescence. By integrating Eq. 2 in the time and frequency spaces, we obtain the following expression for the integrated intensity of the steady-state fluorescence:

$$\begin{aligned} \int_{-\infty}^{+\infty} \mathrm{d}t \int_0^{+\infty} \mathrm{d}\tilde{\nu} R(\tilde{\nu}, t) &= \frac{1}{k_{S2}} \int_0^{+\infty} a_{S2}(\tilde{\nu})\mathrm{d}\tilde{\nu} \\ &\quad + \Phi \frac{k_{S2}}{k_{S2} - k_{S1}} \left(\frac{1}{k_{S1}} - \frac{1}{k_{S2}} \right) \int_0^{+\infty} a_{S1}(\tilde{\nu})\mathrm{d}\tilde{\nu}. \end{aligned} \qquad (3)$$

On the right side of Eq. 3, the first term represents the total intensity of the S_2 fluorescence (I_{S2}), and the second term denotes that of the S_1 fluorescence (I_{S1}). As already mentioned, $a_{S2}(\tilde{\nu})$ and $a_{S1}(\tilde{\nu})$ represent the intrinsic fluorescence transition probability of the S_2 and S_1 state at frequency $\tilde{\nu}$. Thus, the integration of the a_{Si} ($i = 1, 2$) value in the frequency space gives a quantity proportional to the radiative decay rate, and it can be related to the oscillator strength ($\int_0^{+\infty} a_{Si}(\tilde{\nu})\mathrm{d}\tilde{\nu} \propto \tilde{\nu}_{Si}^2 f_{Si}$).[21,27] Consequently, by taking the ratio between I_{S2} and I_{S1}, we obtain the following expression of the quantum yield Φ after a simple calculation:

$$\Phi = \left(\frac{I_{S1}}{I_{S2}} \right) \left(\frac{k_{S1}}{k_{S2}} \right) \left(\frac{\int_0^{+\infty} a_{S2}(\tilde{\nu})\mathrm{d}\tilde{\nu}}{\int_0^{+\infty} a_{S1}(\tilde{\nu})\mathrm{d}\tilde{\nu}} \right) = \left(\frac{I_{S1}}{I_{S2}} \right) \left(\frac{k_{S1}}{k_{S2}} \right) \left(\frac{\tilde{\nu}_{S2}^2}{\tilde{\nu}_{S1}^2} \right) \left(\frac{f_{S2}}{f_{S1}} \right). \qquad (4)$$

Here, $\tilde{\nu}_{Si}$ is the peak frequency of the $S_i \rightarrow S_0$ fluorescence and f_{Si} is the oscillator strength of each transition. The integrated intensities of the S_2 and S_1 fluorescence were obtained from the decomposed steady-state fluorescence spectra and the ratio of I_{S1}/I_{S2} was determined to be 0.032. The oscillator strengths of the $S_2(\pi\pi^*) \leftarrow S_0$ and the $S_1(n\pi^*) \leftarrow S_0$ transitions can be determined from absorption spectra as $f_{S2} = 0.511$ and $f_{S1} = 0.01$, whereas the values of $\tilde{\nu}_{S2} = 25750\ \mathrm{cm}^{-1}$ and $\tilde{\nu}_{S1} = 15000\ \mathrm{cm}^{-1}$ were used as the transition frequencies of the S_2 and S_1 fluorescence. By using these parameters as well as the S_2 and S_1 liferimes ($1/k_{S2} = 0.11$ ps, $1/k_{S1} = 0.50$ ps), we obtained a value of $\Phi = 1.07\ (\pm 0.15)$ for the $S_2 \rightarrow S_1$ electronic relaxation quantum yield. The obtained Φ value can be regarded as unity within error.

The obtained Φ value manifests that the photoexcited S_2 state is almost exclusively relaxed to the "planar" S_1 state. It means that the $S_2 \rightarrow$ "planar" S_1 relaxation process, which we see through time-resolved absorption and Raman spectroscopy, is the major relaxation pathway of the S_2 state. It implies, at the same time, that the rotational isomerization pathway that starts directly from the S_2 state does not exist, or, even if it exists, it is a very minor pathway.

Isomerization Pathway of Photoexcited *trans*-Azobenzene. A series of time-resolved spectroscopies described above gave us a clear and new insight into the photodynamics and photoisomerization process of *trans*-azobenzene. Femtosecond time-resolved absorption study clarified the transient absorption of the S_2 and S_1 states as well as their lifetimes. It

also afforded a direct indication of the production of the *cis* isomer after relaxation of these excited states. Picosecond time-resolved Raman revealed that the observed S_1 state has a "planar" structure and that the relaxation process observed in time-resolved spectroscopy is not the rotational isomerization process but the $S_2 \rightarrow S_1 \rightarrow S_0$ relaxation process occurring in the molecule that essentially retains planarity. This finding indicates that the isomerization starting from the "planar" S_1 state also participates in the photoisomerization after S_2 excitation. Femtosecond time-resolved and steady-state fluorescence study revealed that, in fact, this isomerization pathway, i.e. isomerization in the S_1 state after $S_2 \rightarrow S_1$ relaxation, is the major isomerization pathway following S_2 photoexcitation. It disclosed that the rotational isomerization pathway starting directly from the S_2 state does not exist. Since it has been photochemically demonstrated that the isomerization in the S_1 state occurs by inversion, it can be concluded that the isomerization of azobenzene takes place in the S_1 state by inversion also in the case of S_2 excitation. The "planar" S_1 state observed in time-resolved UV-visible absorption, Raman and fluorescence spectroscopies is assigned to the S_1 state from which the inversion isomerization starts. Figure 7 sketches the isomerization mechanism and the relaxation processes after S_2 excitation, which have been clarified by femtosecond and picosecond time-resolved spectroscopy.

The rotational isomerization pathway starting directly from the S_2 state was originally claimed on the basis of the difference in the isomerization quantum yield between S_2 and S_1 excitation. The isomerization quantum yields have been measured for the S_2 and S_1 excitation in several solvents, and they were reported to be 0.15 (S_2) and 0.28 (S_1) in ethanol, 0.15 and 0.31 in acetonitrile, 0.11 and 0.26 in ethyl bromide, ~0.11 and ~0.24 in isooctane, respectively.[9–11] This difference in the quantum yield had been considered a manifestation of two different isomerization pathways starting from the S_2 and S_1 states. Since the S_2 state is the $\pi\pi^*$ state that induces the rotational isomerization of olefins, it had been believed that the isomerization after S_2 excitation is the rotational isomerization in the S_2 state. However, our studies clearly excluded the existence of this rotational isomerization pathway in the S_2 state. It means that we now need to reconsider the implication of the difference in the isomerization quantum yield between S_2 and S_1 excitation. As discussed in the following, the difference in the isomerization quantum yield suggests that another relaxation channel exists in the vibrationally excited S_1 state.

With the photoexcitation to the S_2 state, molecules gain the energy as high as ~36000 cm^{-1}. After the rapid decay of the S_2 state (0.11 ps), a considerable amount of photoexcited energy is localized in the S_1 state, since the energy dissipation to the surrounding solvents occurs in a much longer time scale (~20 ps[17]). Therefore, an essential difference between S_2 excitation and S_1 excitation is the vibrational excess energy in the "planar" S_1 state that appears after photoexcitation. In other words, the S_1 state that is generated by the $S_2 \rightarrow S_1$ relaxation following the S_2 excitation is very "hot" compared with the S_1 state produced by direct $S_1 \leftarrow S_0$ photoexcitation. Since almost all the S_2 state is relaxed to this "hot" planar S_1 state, the small isomerization quantum yield obtained with S_2 photoexcitation is attributed to the low isomerization efficiency of this vibrationally excited S_1 state. The isomerization quantum yield is determined by the ratio between the rate of isomerization and that of the other relaxation pathway. Therefore, the low isomerization quantum yield implies that the *trans* $S_1 \rightarrow$ *trans* S_0 relaxation process is accelerated in the vibrational excited S_1 state. This argument about the acceleration of the $S_1 \rightarrow S_0$ relaxation process in the vibrationally excited S_1 state is actually consistent with the data of the S_1 lifetime. The lifetime of the S_1 state generated by S_2 excitation (280 nm) was determined to be ~0.5 ps in the present time-resolved fluorescence measurement, whereas the S_1 lifetime measured with the direct red-edge S_1 photoexcitation (503 nm) was reported to be ~2.6 ps.[14] This means that with increase of the vibrational ex-

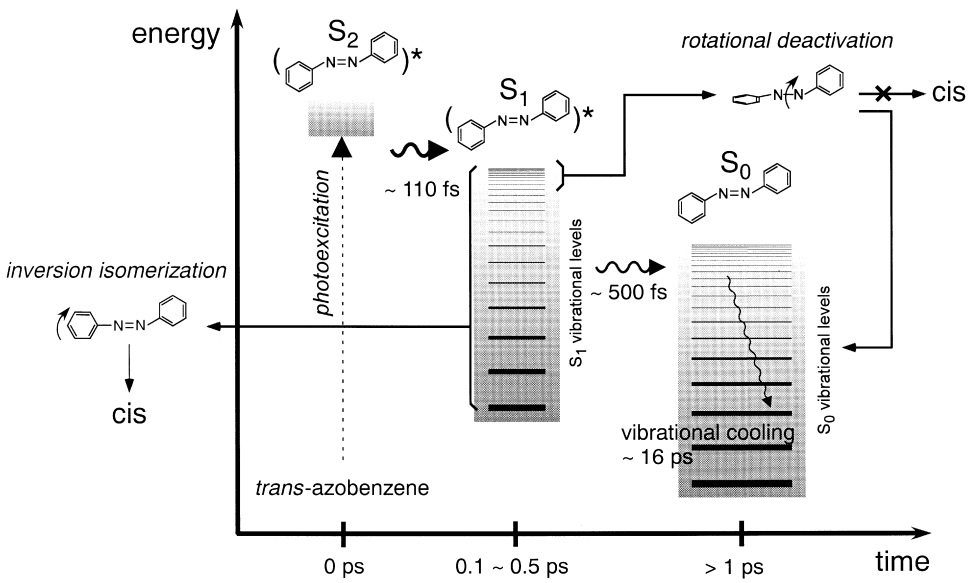

Fig. 7. Schematic diagram of the relaxation and photoisomerization pathway of *trans*-azobenzene after the $S_2(\pi\pi^*) \leftarrow S_0$ photoexcitation in hexane.

cess energy, the S_1 lifetime becomes significantly shorter and the isomerization quantum yield becomes smaller. Such results strongly suggest that a new relaxation channel that accelerates the *trans* $S_1 \rightarrow$ *trans* S_0 relaxation process opens in the vibrationally excited S_1 state.

It has been reported by Rau and Lüddecke that the values of the isomerization quantum yield become the same for S_2 and S_1 excitation when the rotational motion of azobenzene is blocked by chemical modification. They measured the *trans* $\rightarrow$ *cis* isomerization quantum yield of a "blocked" azobenzene and found that the yield remains almost constant even though the excitation condition is significantly changed: 0.21 for the $S_2(\pi\pi^*) \leftarrow S_0$ excitation and 0.24 for the $S_1(n\pi^*) \leftarrow S_0$ excitation. Disapperance of the excess energy dependence was also found in the recent femtosecond time-resolved absorption study reported by Lednev et al.[15] They measured the S_1 lifetime for another rotation-blocked azobenzene after S_2 excitation and found that its lifetime is exactly the same as the lifetime of the S_1 azobenzene that is prepared by the S_1 red-edge excitation (2.6 ps). These facts strongly suggest that the new relaxation channel that opens in the vibrational excited S_1 state is blocked when the rotational motion around the N=N bonding is prohibited. In other words, the new relaxation channel is related to the rotational coordinate, although this relaxation channel finally produces the *trans* S_0 state but does not generate any *cis* isomers. It may be also worth nothing that the statistical distribution of vibrational energy may be not achieved in the vibrationally excited S_1 state where this channel is open. Taking account of the very short lifetime of the S_1 state, especially in hexane (0.50 ps), it is highly likely that the vibrational energy is still localized in particular vibrational modes during the S_1 lifetime. Therefore, it is possible that the rotational deactivation channel, which we discuss here, is open only in the vibrationally excited S_1 state before the intramolecular vibration redistribution (IVR) process.

The time-resolved spectroscopic studies (absorption, Raman and fluorescence) have successfully revealed photochemical dynamics of *trans*-azobenzene following the S_2 photoexcitation. The following new picture has been obtained for the relaxation of the photoexcited azobenzene: After S_2 excitation, first almost all S_2 molecules are relaxed to the S_1 state having a "planar" structure. Then, the S_1 state is relaxed to the S_0 state through the three different relaxation pathways, (1) the inversion isomerization, (2) the *trans* $S_1 \rightarrow$ *trans* S_0 relaxation channel that is open even in the "cold" S_1 state, and (3) the *trans* S_1 $\rightarrow$ *trans* S_0 relaxation channel that is open only in the "vibrational excited" S_1 state. Further elucidation of these three relaxation channels in the S_1 state is necessary for full undrstanding of photochemistry of azobenzene, and, of course, not only experimental studies but also theoretical approaches are highly desirable.

One of the authors, T. F., acknowledges the Japan Society for the Promotion of Science for fellowships. This work was partly supported by the Grants-in Aid for Scientific Research (B) (No. 13440183) snd (C) (No. 1164052) from Japan Society for Promotion of Science, as well as a Grant-in-Aid for Scientific Research on Priority Area (A) (No. 12042283).

References

1 Z. F. Liu, K. Hashimoto, and A. Fujishima, *Nature*, **347**, 658 (1990).
2 Z. Sekkat and M. Dumont, *Appl. Phys. B*, **54** 486 (1992).
3 T. Ikeda and O. Tsutsumi, *Science*, **268**, 1873 (1995).
4 D. H. Waldeck, *Chem. Rev.*, **91**, 415 (1991).
5 J. Saltiel, J. D′Agostino, E. D. Magarity, L. Metts, K. R. Neuberger, M. Wrighton, and O. C. Zafirou, *Org. Photochem.*, **3**, 1 (1973).
6 R. M. Hochstrasser, *Pure Appl. Chem.*, **52**, 2683 (1980).
7 A. Shimojima and T. Tahara, *J. Phys. Chem. B*, **104**, 9288 (2000).
8 H. Rau and E. Lüdecke, *J. Am. Chem. Soc.*, **104**, 1616 (1982).
9 P. P. Birnbaum and D. W. G. Style, *Trans. Faraday Soc*, **50**, 1192 (1954).
10 G. Zimmerman, L. Y. Chow, and U. J. Paik, *J. Am. Chem. Soc.*, **80**, 3528 (1958).
11 P. Bortolus and S. Monti, *J. Phys. Chem.*, **83**, 648 (1979).
12 S. Monti, G. Orlandi, and P. Palmieri, *Chem, Phys.*, **71**, 87, (1982).
13 I. K. Lednev, T.-Q. Ye, R. E. Hester, and J. N. Moore, *J. Phys. Chem.*, **100**, 13338 (1996).
14 I. K. Lednev, T.-Q. Ye, P. Matousek, M. Towrie, P. Foggi, F. V. R. Neuwahl, S. Umapathy, R. E. Hester, and J. N. Moore, *Chem. Phys. Lett.*, **290**, 68 (1998).
15 I. K. Lednev, T.-Q. Ye, L. C. Abbott, R. E. Hester and J. N. Moor, *J. Phys. Chem. A*, **102**, 9161 (1998).
16 T. Nägele, R. Hoche, W. Zinth, and J. Wachtveitl, *Chem. Phys. Lett.*, **272**, 489 (1997).
17 P. Hamm, S. M. Ohline, and W. Zinth, *J. Chem. Phys.*, **106**, 519 (1997).
18 T. Fujino and T. Tahara, *J. Phys. Chem. A*, **104**, 4203 (2000).
19 T. Fujino, S. Y. Arzhantsev, and T. Tahara, *J. Phys. Chem. A*, **105**, 8123 (2001).
20 S. C. Jeoung, S. Takeuchi, T. Tahara, and D. Kim, *Chem. Phys. Lett.*, **309**, 369 (1999).
21 S. Takeuchi and T. Tahara, *J. Phys. Chem. A*, **101**, 3052 (1997).
22 S. Y. Arzhantsev, S. Takeuchi, and T. Tahara, *Chem. Phys. Lett.*, **330**, 83 (2000).
23 L. F. Feser, and K. L. Williamson, "Organic Experiments 4th ed," Maruzen. Tokyo (1980).
24 J. Azuma, N. Tamai, A. Shishido, and T. Ikeda, *Chem. Phys. Lett.*, **288**, 77 (1998).
25 The contribution from the *cis* isomer (photoproduct) is very small at 405 nm, so that we fitted the observed decay by a double exponential function, neglecting the long-lived component.
26 D. R. Armstrong, J. Clarkson, and W. E. Smith, *J. Phys. Chem.*, **99**, 17825 (1995).
27 N. J. Turro, "Molecular Photochemistry," W. A. Benjamin Inc., Massachusetts (1965).